Effect of temperature on the working stroke of muscle myosin

V. Decostre*, P. Bianco, V. Lombardi, and G. Piazzesi†

Laboratory of Physiology, Dipartimento di Biologia Animale e Genetica, Università degli Studi di Firenze, Via G. Sansone 1, 50019 Sesto Fiorentino, Italy

Communicated by Edwin W. Taylor, Northwestern University Feinberg School of Medicine, Chicago, IL, August 14, 2005 (received for review April 12, 2005)

Muscle contraction is due to myosin motors that transiently attach with their globular head to an actin filament and generate force. After a sudden reduction of the load below the maximum isometric force (T_0), the attached myosin heads execute an axial movement (the working stroke) that drives the sliding of the actin filament toward the center of the sarcomere by an amount that is larger at lower load and is 11 nm near zero load. Here, we show that an increase in temperature from 2 to 17°C, which increases the average isometric force per attached myosin head by 60%, does not affect the amount of filament sliding promoted by a reduction in force from T_0 to $0.7T_0$, whereas it reduces the sliding under low load by 2.5 nm. These results exclude the possibility that the myosin working stroke is due to the release of the mechanical energy stored in the initial endothermic force-generating process and show that, at higher temperatures, the working stroke energy is greater because of higher force, although the stroke length is smaller at low load. We conclude the following: (*i*) the working stroke is made by a series of state transitions in the attached myosin head; (*ii*) the temperature increases the probability for the first transition, competent for isometric force generation; and (*iii*) the temperature-dependent rise in work at high load can be accounted for by the larger free energy drop that explains the rise in isometric force.

muscle contraction | muscle energetics | myosin working stroke

Force and shortening in muscle are generated by cyclical interactions between the globular part of the myosin molecule (the myosin head) extending from the thick myosin filament and the thin actin filament. During each interaction, an interdomain structural change in the myosin head (the working stroke) produces a pull on the actin filament toward the center of the myosin filament, while one molecule of ATP is hydrolyzed (1, 2). The reduction of force from the steady isometric force T_0 to a load T induces a two-phase response in the attached myosin heads: first the instantaneous recoil of the elasticity in the myofilaments and in the myosin heads (phase 1) and then the rapid isotonic shortening due to the synchronous execution of the working stroke in the attached myosin heads (phase 2). Because phase 2 shortening occurs under isotonic conditions, it is not influenced by the myofilament compliance, and its amount (L_T) directly measures the size of the myosin working stroke under the load T (3, 4).

A rise in temperature increases the isometric force developed on average by an attached myosin head (5), revealing the endothermic nature of isometric force generation (6–12). In contrast, shortening is known to be exothermic (13–16), but the temperature dependence of the steps involved in the execution of the working stroke itself is not known. Because the chemomechanical transduction process is unique, we could expect that the thermal energy captured in the reaction responsible for isometric force determines the energy released during the working stroke driving filament sliding at loads $< T_0$ and thus that both force and shortening increase with temperature.

Here, we determine the dependence on temperature (range 2–17°C) of L_T after force steps from T_0 to T in the range 0.7–0.1 T_0. The results show that (*i*) at $0.7T_0$, L_T (4.5–4.8 nm) is not substantially affected by temperature, and the isotonic work W_T ($= L_T \cdot T$) rises by ≈50%, in accordance with the increase in the free energy change that explains the rise in T_0 (5); and (*ii*) at $0.1T_0$, L_T reduces from 7.4 to 4.9 nm with the increase in temperature, showing that the rise in isometric force with temperature occurs at the expense of the early steps of the same series of state transitions driving the working stroke.

Methods

Fiber Preparation and Mechanical Apparatus. Single fibers were dissected from the lateral head of the tibialis anterior muscle of *Rana esculenta* after killing by decapitation followed by destruction of the brain and the spinal cord (European Economic Community Directive 86/609/EEC). Fibers were transferred to a thermoregulated trough and mounted between a capacitance force transducer with resonance frequency ≈50 kHz (17) and a loudspeaker motor (18), by means of aluminum clips fixed to the tendons (6). Sarcomere length was set at 2.15 μm. The loudspeaker motor was servo-controlled by using as feedback signal the output from either the position sensor of the motor lever (fixed-end mode) or the force transducer (force-clamp mode). A striation follower (19) continuously recorded the sarcomere length changes in a 1- to 1.5-mm segment at the fiber end close to the force transducer with a sensitivity of 100 mV·nm^{-1} per half-sarcomere (hs).

The physiological solution bathing the fiber (115 mM NaCl/2.5 mM KCl/1.8 mM $CaCl_2$/3 mM phosphate buffer, pH 7.1) was kept at the chosen temperature by means of a servo-controlled thermoelectric module. The mechanical protocol described below was repeated on each fiber at four different temperatures, 2, 5, 10, and 17 ± 0.1°C, at random.

Experimental Protocol. Fibers were stimulated isometrically under fixed-end mode by means of platinum plate electrodes to produce a fused tetanus. Tetanus duration, stimulus frequency, and time interval between tetani were adjusted at the different temperatures as described in ref. 5. When force had reached the tetanic plateau (T_0), control was shifted from fixed-end to force-clamp mode. A step to a force $T < T_0$ was imposed 2 ms later by using as a command the output of an integrated circuit that generated steps to a preset fraction of T_0 (range 0.1–0.9). The time resolution of our load clamp system (3) is adequate to impose steps in force complete within 140 μs, so that in the resulting velocity transient (Fig. 1*A*; see also refs. 20 and 21) the early isotonic shortening (phase 2) can be separated from the elastic response (phase 1). The control was switched back to fixed-end mode during the latter steady shortening phase (phase 4). The response to $0.9T_0$ was sometimes oscillatory (22), and we limited the analysis presented here to data from 0.1 to 0.7 T_0.

For each fiber, we determined the isotonic velocity transient

Abbreviations: hs, half-sarcomere; zJ, zeptojoule.

*Present address: Institut National de la Santé et de la Recherche Médicale UR582, Institut de Myologie, 75651 Paris Cedex 13, France.

†To whom correspondence should be addressed. E-mail: gabriella.piazzesi@unifi.it.

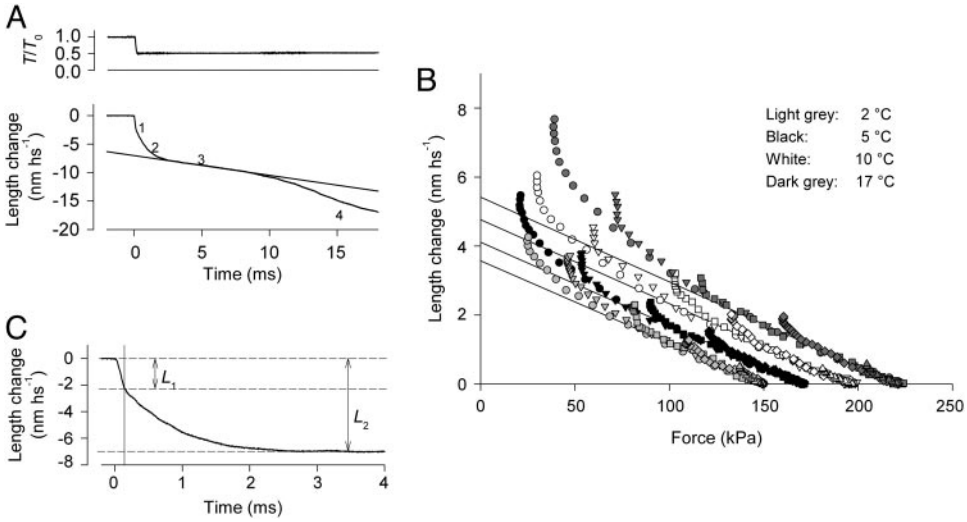

Fig. 1. Estimates of the elastic and working stroke response in the velocity transient. (*A*) Velocity transient (lower trace) after a step in force (upper trace) from the isometric tetanic value (T_0) to $0.5T_0$. The four phases of the velocity transient are indicated by the numbers close to the length trace. The straight line is the fit to the linear part of phase 3. (*B*) Instantaneous length–force relations during force steps of different size, as indicated by symbols, at 2°C (light gray), 5°C (black), 10°C (white), and 17°C (dark gray). Continuous lines are the regressions to the initial linear portions of the relations. Regression equation is $L_1' = Y_0 - 1/E{\cdot}T$, where Y_0 is the ordinate intercept (nm·hs^{-1}), T is the force (kPa), and E is the Young modulus (MPa). (*C*) Time course of the early shortening (phases 1 and 2 as indicated by the labels), after subtraction of the line fitted to phase 3 as in *A*.

for four different loads, 0.1, 0.3, 0.5, and 0.7 T_0, at four different temperatures, 2, 5, 10, and 17°C. Data reported here refer to only four fibers (of the 13 fibers used for these experiments) on which we succeeded in completing the protocol.

A multifunction input/output board (PCI-6110E, National Instruments, Austin, TX) and a program written in LABVIEW (National Instruments) were used to record outputs from the force transducer, the striation follower, and the loudspeaker motor. To resolve the early phases of the isotonic velocity transient, the acquisition rate was 200 kHz.

Data Analysis

Measurements of the Elastic Response. Because phases 1 and 2 of the velocity transient (Fig. 1*A*) have the same polarity, the shortening attained at the end of phase 1 elastic response, L_1, is influenced by the contribution of phase 2 shortening that begins during the step itself. The effect of phase 2 can be subtracted from the phase 1 response by back-extrapolating the tangent to the first part of phase 2 to the half-time of the step (figure 1*C* in ref. 3). Alternatively the elastic response can be measured by plotting the instantaneous length–force relations during the step itself. This method resulted more reliable at high temperature, where the very high speed of phase 2 shortening smoothes the angle in the length trace at the end of force step. Instantaneous length–force plots from a fiber are shown in Fig. 1*B* for steps of different sizes at the four temperatures used. At each temperature, responses to different step sizes superimpose for the first part, as expected from a pure elasticity, and then deviate near the end of phase 1 due to the contribution of phase 2 shortening. Continuous lines are the linear regressions to the pooled data up to half of the force drop. The regression equation at each temperature is used to calculate L_1', the length change due to the elastic response for each force step.

Measurement of the Amplitude (L_T) and Rate (r) of the Isotonic Working Stroke. Phase 2 shortening is the mechanical manifestation of the working stroke in the attached myosin heads and is followed by a pause (phase 3, Fig. 1*A*) that is due to detachment/reattachment of heads (4). The amplitude of the shortening attained at the end of phase 2 (L_2) is estimated by subtracting the linear regression equation fitted to phase 3 from the early phases of the velocity transient (Fig. 1*C*). L_2 is the sum of the elastic response plus the working stroke response occurring in isotonic conditions; thus, for each clamped force T, the size of the isotonic working stroke, L_T, is obtained by subtracting the elastic response L_1' from L_2. The time course of the isotonic working stroke exhibited an almost exponential shape, therefore the speed of the process (r) was estimated by the reciprocal of the time from the end of the step (140 μs after the step start, when the length attains L_1) to 63% of $L_2 - L_1$.

Results

Effect of Temperature on the Size of the Working Stroke. Rise of temperature from 2 to 17°C increased the isometric tetanic force (T_0) by ≈60% (Table 1), in agreement with previous results (5). A step reduction in force to $T < T_0$ elicited an isotonic velocity transient made of the following four phases (Fig. 1*A*; refs. 3, 20, and 21): phase 1, the drop in length simultaneous with the force step that reflects the hs elasticity; phase 2, the early rapid shortening due to the working stroke in the attached myosin heads; phase 3, the subsequent reduction of the shortening velocity, related to detachment of the heads attached in the original isometric condition and attachment farther along the actin filament (4, 23); and phase 4, the final shortening at constant velocity related to steady-state detachment/attachment of heads.

The effects on the velocity transient of the increase in temperature from 2 to 17°C are shown in Fig. 2*A* for a force drop to $0.5T_0$: with temperature rise the speeds of shortening in phase 2 and 4 become faster and phase 3 become briefer.

The instantaneous elasticity of the hs is estimated from the length–force plots during the step (Fig. 1*B*). The L_1' lines in Fig. 2*B* are the regression lines to data points as in Fig. 1*B* but from another fiber. In both cases the lines exhibit almost the same slope independently of the temperature, indicating that the hs stiffness (measured by the Young modulus E, Table 1) is not affected by temperature (5). Therefore, the hs strain at T_0, Y_0 (measured by the ordinate intercept of the L_1' lines, Figs. 1*B* and 2*B*), increases in proportion with the increase in isometric force (Table 1). This result indicates that both the passive elements of

Table 1. Temperature dependence of isometric force, stiffness, hs strain, free-energy change, and average isometric strain and force per head

Temp., °C	T_0,* kPa	Relative force,† $T_{0,t}/T_{0,2}$	E,‡ MPa	Y_0,§ nm·hs^{-1}	ΔG,¶ zJ	s,‖ nm	F_0,‖ pN
2	144 ± 11	1	41.24 ± 4.29	3.49 ± 0.24	−0.5	1.46	4.53 ± 0.38
5	172 ± 8	1.19 ± 0.11	43.03 ± 2.87	4.01 ± 0.18	−1.62	1.74	5.39 ± 0.45
10	197 ± 12	1.37 ± 0.13	41.60 ± 3.15	4.75 ± 0.23	−3.49	2.00	6.20 ± 0.52
17	226 ± 14	1.57 ± 0.15	38.54 ± 3.01	5.88 ± 0.29	−6.11	2.29	7.11 ± 0.60

*Means ± SE of absolute isometric force.
†Means ± SE of isometric force relative to the value at 2°C.
‡Means ± SE of Young modulus (given by the slope of the L_1' line).
§Means ± SE of strain of the hs at T_0.
¶The free energy change, calculated fitting Eq. **1** to T_0:1/θ relation. The fit on the four temperature (2–17°C) points was constrained by taking for $T_{0,max}$ the value estimated in ref. 3 on the five temperature points. ΔH and ΔS from these data are 102.42 ± 8.87 zJ and 0.374 ± 0.032 zJ/K, respectively.
‖The average isometric strain (s) and force (F_0) per head. The error of F_0 is propagated from that of the head stiffness (ε) (see text).

the hs, the myofilaments, and the active elements, the attached myosin heads, are strained in proportion with force. Thus, the rise in force with temperature is explained by a corresponding increase in average force per attached myosin head (5).

L_2, the amount of filament sliding at the end of phase 2, is the sum of the elastic response and the working stroke response (see Fig. 1*C* and *Methods*). The effect of temperature on L_2 is shown by symbols in Fig. 2*B*. The intercept of the L_2 relation on the length axis (that represents the maximum extent of filament sliding accounted for by the attached heads) is not significantly affected by temperature (11.17 ± 0.63 and 10.62 ± 0.46 nm at 2 and 17°, respectively). The L_2–T points at any relative load are shifted to the right in proportion to the temperature-dependent increase in force, without a significant change in L_2 (Fig. 2*B*). Consequently, the slope of the L_2 relations progressively reduces with the rise in temperature. The isotonic working stroke, L_T, is calculated from the difference $L_2 - L_1'$ (Fig. 2 *B* and *C*). At each temperature, L_T increases as the load relative to T_0 reduces (as previously found at 4°C; dashed line in Fig. 2*C* from figure 2*B* in ref. 3), but the slope of the $L_T - T/T_0$ relation progressively reduces as temperature increases. Thus, the increase of temperature reduces L_T at low loads much more than at high loads: at $0.1T_0$, L_T reduces from 7.39 ± 0.53 nm at 2°C to 4.94 ± 0.54 nm at 17°C ($P < 0.01$), whereas at $0.7T_0$, the change of L_T from 4.77 ± 0.30 nm at 2°C to 4.45 ± 0.30 nm at 17°C is not significant ($P > 0.15$).

The mechanical work (W_T) delivered during the isotonic working stroke is calculated by the product L_T·T. W_T increases

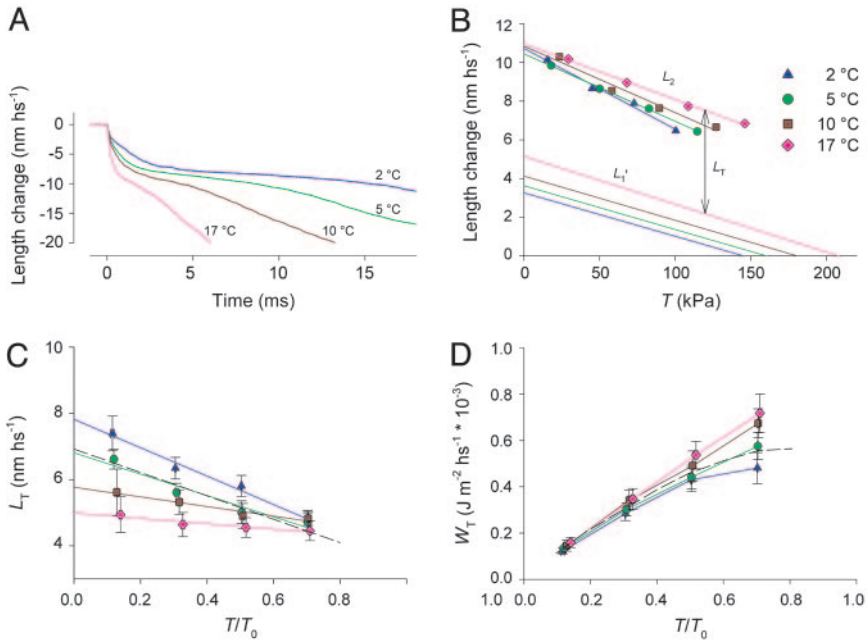

Fig. 2. Effect of temperature on the elastic and working stroke response. (*A*) Velocity transients after a force step to $0.5T_0$ at the four different temperatures, 2°C (blue), 5°C (green), 10°C (brown), and 17°C (pink). (*B*) L_1' and L_2 relations vs. the clamped force T (kPa) at the four temperatures as indicated by the same color code as in *A*. For clarity, L_1' relations are represented by the regression lines fitted to data points as explained in *Methods*, and L_2 relations are represented by the points and by the corresponding regression lines. L_T is obtained by subtracting L_1' from L_2 for each T. (*C*) L_T:T/T_0 relations (means ± SE, four fibers) at the four temperatures as indicated by the same colors as in *B*. T_0 is the isometric tetanic force at the corresponding temperature. Continuous lines are the linear regression equations fitted to the mean points at each temperature. The dashed line is the regression line for the L_T:T/T_0 relation at 4°C reported as open circles in figure 2*B* of ref. 3. (*D*) Relations between the mechanical energy during the isotonic working stroke (W_T) and T/T_0. Mean data points are joined by lines. The dashed line is obtained by joining the data at 4°C reported as filled circles in figure 2*B* of ref. 3.

with the load up to a maximum attained at 0.7–0.8 T_0 (3). Temperature increases W_T at any load (symbols in Fig. 2*D*), but the effect is larger at high loads than at low loads: from 2 to 17°C, W_T increases by 30% at $0.1T_0$ (from 0.122 ± 0.015 J·m^{-2}·hs^{-1} × 10^3 to 0.159 ± 0.022 J·m^{-2}·hs^{-1} × 10^3) and by 50% at $0.7T_0$ (from 0.481 ± 0.067 J·m^{-2}·hs^{-1} × 10^3 to 0.719 ± 0.082 J·m^{-2}·hs^{-1} × 10^3). Consequently, the slope of the $W_T - T/T_0$ relation is greater the higher the temperature. The larger increase of W_T at high relative forces is accounted by the increased force because the value of L_T is almost the same at both temperatures (Fig. 2*C*).

Effect of Temperature on the Rate of the Working Stroke. The time course of phase 2 shortening, isolated by subtracting the linear component of phase 3 (Fig. 1 *A* and *C*), is roughly exponential, and its speed can be defined by the reciprocal (r) of the time to 63% of its completion (see *Methods*). At each temperature, r increases as the load decreases (see also ref. 3) and, at a given relative load, is larger at higher temperature (Fig. 2*A*). The temperature dependence of r at each load is shown in Fig. 3*A* by plotting ln r against the reciprocal of the absolute temperature, $1/\theta$. Because the temperature-dependent forward shift in the state distribution of cross-bridges is associated to increase in r (5), we attribute it to an increase in the rate of forward transition. Consequently, the plots in Fig. 3*A* are considered a good approximation of Arrhenius relation for the forward rate constant, $\ln r = \ln A - E_a/k_B\theta$, where E_a, proportional to the slope of the relation, is the activation energy of the forward state transition, A is the preexponential factor (or frequency factor), and k_B is the Boltzmann constant. The plots are shifted upward with the reduction of the load. E_a is ≈110 J × 10^{-21} (zeptojoule; zJ) at $0.7T_0$ and slightly reduces (≤10%), with the reduction of the load, with the exception of $0.1T_0$ (see legend in Fig. 3*B*). The interpretation of these changes in E_a has limitations that are considered in *Discussion*.

Discussion

The increase in T_0 by temperature at constant stiffness confirms the conclusion of length step experiments (5) that temperature increases the average force per attached myosin head by controlling the equilibrium distribution between low-force and high-force-generating states of the attached myosin heads.

Here, we find that the maximum amount of sliding accounted for by the attached myosin heads, measured by the abscissa intercept of the L_2 curve, is ≈11 nm independent of temperature (Fig. 2*B*). This value is the sum of the axial motion elicited under zero load and of the recoil of the elastic elements that corresponds to the working stroke expended in straining the same elastic elements at T_0 (24). A maximum working stroke of 11 nm matches the structural constraints suggested by the crystallographic model (4, 25–27).

After subtracting the elastic shortening (L_1') from L_2, the isotonic working stroke at low loads ($0.1T_0$) is ≈7.5 nm at 2°C and ≈5 nm at 17°C. The reduction corresponds to the increased T_0 strain at the higher temperature (Y_0; Table 1), indicating that the process responsible for the isometric force generation is modulated by temperature at the expenses of the same state transitions responsible for the working stroke that drives filament sliding.

At higher loads the working stroke is smaller and slower than at low loads (4, 5). This feature can be explained in terms of Huxley and Simmons (28) model of force generation (see also the state diagrams shown in Fig. 3 *B* and *C*). A basic assumption for the application of the model is that the transitions between attached states of the myosin heads are rapid enough that the rates of heads entering or leaving the equilibrium mixture are negligible. According to the model, in the isometric condition there is an equilibrium between different force-generating states of the attached heads due to the balance between the basic free energy difference that drives the forward transition and the mechanical energy that accumulates in the elasticity (Fig. 3*B*). At low temperature (Fig. 3*C*, continuous line) the equilibrium is

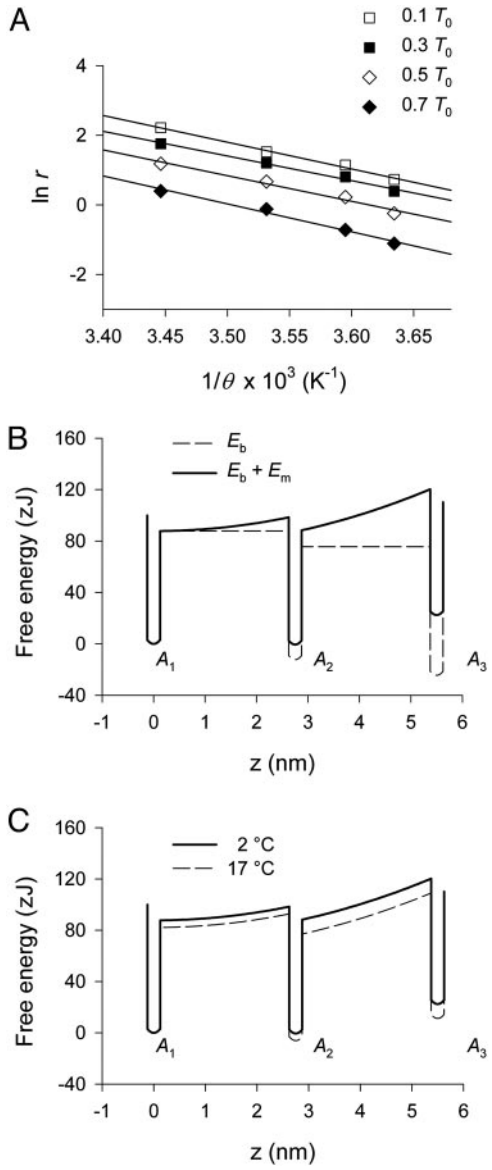

Fig. 3. Estimate of the activation energy and free energy profiles of the cross-bridge states. (*A*) Relation between ln r and $1/\theta$, the reciprocal of the absolute temperature at the four loads as indicated by the symbols in the legend. Continuous lines are the linear regression equations fitted to data. The slopes of the relations, which estimate the activation energy (E_a), are 111 ± 9 zJ at $0.7T_0$; 102 ± 11 zJ at $0.5T_0$; 98 ± 7 zJ at $0.3T_0$; and 106 ± 6 zJ at $0.1T_0$. *B* and *C* show the free energy profile assumed for the first two transitions between states A_1, A_2, and A_3 of the attached myosin heads and the effect of temperature. (*B*) Profile of the basic free energy (E_b, dashed line) and of the total free energy in isometric conditions ($E_b + E_m$, continuous line) at 2°C. The energy profiles are represented as a function of the coordinate z, the extent of the structural transition responsible for the working stroke that, in isometric conditions, represents also the strain (s) generated in the head by the transition. For simplicity it is assumed that: (*i*) z is the same for either transition $A_1 \rightarrow A_2$ or $A_2 \rightarrow A_3$, so that, in isometric conditions, $z = s_{A_2} = 2.75$ nm and $s_{A_3} = 5.50$ nm, as explained in the text; and (*ii*) ΔE_b for either transition ($E_{b,A_i} - E_{b,A_{i-1}}$) at a given temperature is the same: at 2°C ΔE_b is 12.22 zJ and at 17°C it is 17.83 zJ. (*C*) Comparison of free energy profiles at 2°C (continuous line) and at 17°C (dashed line). The increase in ΔE_b with temperature is represented as a reduction in the activation energy for the forward transition according to the finding that the rate of state transition after length steps (ref. 5) or force steps (*A*) increases with temperature.

such that 50% of the attached heads are in a low force state (A_1) and 50% in a high force state (A_2); the increase of temperature shifts the equilibrium toward the high force state by decreasing its basic free energy. This shift of the equilibrium results in a larger average strain of the head as temperature increases.

A drop in force that reduces the mechanical energy barrier promotes a forward shift in the equilibrium distribution. The extent of the state transitions (or working stroke) depends on the load at which the force is clamped: at zero load (represented by dashed line in Fig. 3*B*) the myosin heads go through all of the transitions, causing a filament sliding corresponding to the working stroke not consumed during the state transitions leading to the isometric state equilibrium, so that the working stroke is shorter as the temperature increases; at high load most of the heads attain a new equilibrium distribution at an intermediate stage of the working stroke, from which they detach.

At the higher temperature the stroke occurs at a higher level of force per myosin head, increasing the work W_T. Because (*i*) the number of attached heads is not changing with temperature and (*ii*) the work per head is the integral of the force with respect to sliding distance covered while it is attached, it follows that the increase in W_T indicates a corresponding increase in efficiency of energy conversion.

Thermodynamic Basis of the Temperature-Dependent Increase in Force and Work. W_T increases with temperature, and the increase is larger at the higher loads, i.e., in the region of maximal efficiency of shortening muscle (16). This result suggests that the state transitions responsible for the working stroke have the same endothermic nature as that found for isometric force generation (5). In that case, the rise in force with temperature was explained with a forward shift of the equilibrium between two states of the attached myosin heads, A_1 (with force $F_{A_1} = 0$) and A_2 (with force F_{A_2}), driven by a temperature-dependent increase of free-energy change (ΔG). The relation of T_0 (range 2–24°C) vs. $1/\theta$ (the reciprocal of absolute temperature) was fitted by the equation (derived from van't Hoff equation)

$$T_{0,t} = T_{0,max}/(1 + \exp(\Delta H/k_B\theta - \Delta S/k_B)), \qquad [1]$$

where $T_{0,t}$ is the isometric force at temperature t, $T_{0,max}$ is the maximum isometric force, ΔH is the enthalpy change, k_B is the Boltzmann constant, ΔS is the entropy change, and $\Delta H - \theta\Delta S = \Delta G$. The result of the fit indicated the following: (*i*) $T_{0,max} \approx 280$ kPa; (*ii*) at 2°C the change in the entropic factor, $\theta\Delta S$, becomes almost equal to ΔH, thus $\Delta G = 0$ and the ratio $n_2/(n_1 + n_2)$ (the number of A_2 heads over the total number of attached heads) = 0.5; and (*iii*) as temperature increases, $\theta\Delta S$ increases, determining the drop in ΔG that promotes the forward shift in the equilibrium distribution (table 2 of ref. 5). The conclusion that at 2°C the equilibrium constant of the force-generating transition is nearly one indicates that the mechanical energy of the A_2 state (E_{m,A_2}) just balances the drop in basic free energy ($E_{b,A_2} - E_{b,A_1}$) of the transition $A_1 \rightarrow A_2$.

We have applied the same kind of analysis to the results in this work and have obtained the temperature dependence of ΔG reported in Table 1. The value of -0.5 zJ at 2°C corresponds to a fraction of 0.53 heads in state A_2, confirming that at 2°C the equilibrium constant of the $A_1 \rightarrow A_2$ transition is nearly one, and therefore the mechanical energy of the A_2 state (E_{m,A_2}) is similar to the drop in the basic free energy ($E_{b,A_2} - E_{b,A_1}$) of the transition (Fig. 3*B*). The change in ΔG with temperature (Table 1) provides an estimate of the mechanical energy accumulated in the elasticity in isometric conditions at any temperature, from which the stiffness ε of the attached myosin heads can be calculated

$$\varepsilon = 2\Delta G_{t_2-t_1}/({s_{t_2}}^2 - {s_{t_1}}^2), \qquad [2]$$

where $\Delta G_{t_2-t_1}$ is the change in free energy drop with the rise from temperature t_1 to temperature t_2 (that corresponds to the change in mechanical energy E_{m,t_2-t_1}) and s_{t_1} and s_{t_2} are the average strains per attached head at t_1 and t_2, respectively. s at any given temperature (Table 1) can be calculated from the corresponding hs strain, Y_0, taking into account the contributions due to the compliances of the actin and myosin filaments (see *Supporting Text*, which is published as supporting information on the PNAS web site). With ΔG and s from Table 1 and $t_1 = 2$°C, the average value of ε calculated for the three t_2 values (5, 10, and 17°C) with Eq. **2** is 3.10 ± 0.26 pN·nm^{-1}. Consequently, the average isometric force per attached head ($F_0 = s{\cdot}\varepsilon$) can be derived for the four temperatures (Table 1). Note that the change in s and F_0 with temperature is because of the change in equilibrium constant of the transition between states, not because s and F_0 in a state is temperature dependent.

Fig. 3*B* shows isometric state diagrams representing the free-energy profiles of states A_1, A_2, and A_3 of the attached myosin heads as a function of the transition coordinate z (actually, as discussed later, there are likely more than two state transitions). The diagrams are illustrative and therefore do not give realistic profiles along the reaction coordinate. Comparison of free-energy profiles at 2 and 17°C is shown in Fig. 3*C*.

The purpose of the diagrams is to illustrate that in isometric conditions force generation is due to the equilibrium distribution between the first two attached states: at 2°C the equilibrium constant of the $A_1 \rightarrow A_2$ transition is nearly 1, and raising the temperature produces only a shift in the equilibrium distribution between these two states, whereas the second transition remains absolutely unfavorable.

Because we assumed that the force in A_1 state (F_{A_1}) and thus the strain (s_{A_1}) are zero, knowing the fractional distribution of heads between A_1 and A_2 state, we can calculate the isometric strain in A_2 state, s_{A_2} [$= s/(n_2/(n_1 + n_2))$] = 2.75 nm, which corresponds to the extent of the structural change z associated with the transition (Fig. 3*B*).

With the above values of s_{A_2} and ε, the isometric force of A_2 state ($F_{A_2} = \varepsilon{\cdot}s_{A_2}$) and its isometric mechanical energy ($E_{m,A_2} = 1/2\varepsilon{\cdot}s_{A_2}^2$) are 8.52 pN and 11.72 zJ respectively. Thus, the mechanical energy for the first transition is a relatively small component of the activation energy for the transition, ≈100 zJ, as estimated in this work and in ref. 5.

Dependence of the Working Stroke Size on Temperature and Load. With the rise in temperature, the level of E_{b,A_2} drops, producing the corresponding increase in ΔG that drives the shift in the equilibrium distribution toward the A_2 state (Fig. 3*C*). However the rise in temperature cannot *per se* induce a second step in the working stroke. In fact, in isometric conditions, the mechanical energy of A_3 state [$E_{m,A_3} = (1/2)\varepsilon{\cdot}s_{A_2}^2$] is 46.89 zJ (Fig. 3 *B* and *C*), 35 zJ above that of the A_2 state and one order of magnitude larger than the drop in ΔG between 2 and 17°C (5.61 zJ from Table 1). Thus, also at 17°C the free energy change of the transition $A_2 \rightarrow A_3$ is unfavorable by ≈30 zJ (7 $k_B\theta$).

State transitions beyond that responsible for isometric force generation occur only if the mechanical energy barrier is reduced by a drop in force. The extent of this progression in the working stroke depends on the load to which the force is clamped. In fact, the transitions are continuously powered through the working stroke by the consecutive drops in E_b and stop when the total change in E_b is equilibrated by E_m for that load: the stop occurs after a smaller number of transitions at higher loads and never occurs at low loads at which the transitions progress to the final state. Under these conditions, an increase in temperature, which increases ΔE_b of each transition, shifts forward the state distribution for which E_m equilibrates the total change in E_b. This consideration explains the temperature-dependent increase in the isotonic work produced at high load (Fig. 2*C*). With F_0 and

L_T at 0.7 the isometric force, we can calculate the isotonic work per head at maximum efficiency ($w_{max} = 0.7\ F_0 \cdot L_{T(0.7)}$). w_{max} = 15.11 zJ at 2°C and rises to 22.11 zJ (+46%) at 17°C. ΔE_b for each transition is 12.22 zJ at 2°C and (12.22 + 5.61 =) 17.83 zJ (+46%) at 17°C. Thus, the increase in w_{max} with temperature is explained by the increase in the basic free-energy change between states. Moreover, because at each temperature ΔE_b for one transition is smaller than w_{max}, it can be concluded that also at the higher loads the working stroke elicited by a drop in force progresses for more than one transition.

The two conclusions above indicate that not only the early force-generating step but the whole conformational change within the motor domain of the myosin head is characterized by entropy-driven hydrophobic interactions.

Load Dependence of the Activation Energy. The rise in temperature increases the speed of the working stroke at each load (Fig. 3*A*). The Arrhenius plots are shifted downward by the increase of the load with minor changes in the slope, indicating an activation energy (E_A) of the working-stroke reaction of ≈100 zJ. This value, which corresponds to $Q_{10} \approx 2.5$, found for the speed of quick force recovery after length steps (5, 6, 29), is used for the energy wells in Fig. 3 *B* and *C*. However, it must be taken into account that these Arrhenius plots are the result of a rough approximation, because we demonstrate that the working stroke is made by a series of state transitions and that at low load the number of transitions is smaller at high temperature than at low temperature (this work and refs. 3–5). As a consequence, in Fig. 3*A*, the leftmost and the rightmost open squares would shift upward and downward, respectively, producing an overestimate of the slope of the Arrhenius plot and of the activation energy at $0.1T_0$.

The energy profiles assumed in the model in Fig. 3*B* and *C* to explain the temperature dependence of the force and isotonic work per myosin head indicate that in isometric conditions E_m is only 1/10 of the activation energy for the forward state transition. Therefore, the effect on the activation energy of the reduction of the load is expected to be small as observed.

Suggestions for the Working Stroke Model. Our conclusion that the working stroke in the myosin head is made by multiple state transitions that progress by different amounts depending on the mechanical conditions challenges the view from crystallographic models of a switch-like conformational change promoted by the release of ATP hydrolysis products. Instead, our conclusion provides the right constraints for a kinetic–mechanical model of the working stroke that must incorporate the finding that the average isometric strain in the myosin head, 1.5–2.3 nm (Table 1), is 13–21% the maximum structural change. Thus, the mechanical energy liberated with the working stroke must be partitioned in several steps powered by subsequent state transitions. With a transition step size (z) of 2.75 nm (Fig. 3*B*), four steps are requested to complete the maximum structural change of 11 nm. Accordingly the mechanical energy of the transition responsible for isometric force generation (E_{m,A_2}), 12 zJ (or 3 $k_B\theta$), is ≈1/8 of the free energy of the ATP hydrolysis or ≈1/4 of the maximum mechanical energy liberated in one actin–myosin interaction with the known muscle efficiency (50%).

The finding that force generation in isometric conditions implies a drop of free energy of ≈1/8 of the free energy of the ATP hydrolysis indicates that myosin heads can form strong force-generating interactions with actin at an early stage of the chemomechanical transduction cycle. This conclusion supports the view that the release of the first of the ATP hydrolysis products, inorganic phosphate, which implies a large enthalpy change (30), can follow the formation of the strong force-generating actin–myosin interaction (31).

We thank Prof. R. Woledge for stimulating discussion and comments and Mr. A. Aiazzi and Mr. M. Dolfi for technical assistance. This work was supported by Ministero Istruzione, Università e Ricerca (Italy, Cofin 2002), National Institutes of Health Grant R01AR049033-01, and European Union Grant HPRN-CT-2000-00091.

1. Huxley, A. F. (1957) *Prog. Biophys. Biophys. Chem.* **7,** 255–318.
2. Lymn, R. W. & Taylor, E. W. (1971) *Biochemistry* **10,** 4617–4624.
3. Piazzesi, G., Lucii, L. & Lombardi, V. (2002) *J. Physiol. (London)* **545,** 145–151.
4. Reconditi, M., Linari, M., Lucii, L., Stewart, A., Sun, Y. B., Boesecke, P., Narayanan, T., Fischetti, R. F., Irving, T., Piazzesi, G., *et al.* (2004) *Nature* **428,** 578–581.
5. Piazzesi, G., Reconditi, M., Koubassova, N., Decostre, V., Linari, M., Lucii, L. & Lombardi, V. (2003) *J. Physiol. (London)* **549,** 93–106.
6. Ford, L. E., Huxley, A. F. & Simmons, R. M. (1977) *J. Physiol. (London)* **269,** 441–515.
7. Ranatunga, K. W. & Wylie, S. R. (1983) *J. Physiol. (London)* **339,** 87–95.
8. Goldman, Y. E., McCray, J. A. & Ranatunga, K. W. (1987) *J. Physiol. (London)* **392,** 71–95.
9. Bershitsky, S. Y. & Tsaturyan, A. K. (1992) *J. Physiol. (London)* **447,** 425–448.
10. Davis, J. S. & Harrington, W. F. (1993) *Biophys. J.* **65,** 1886–1898.
11. Zhao, Y. & Kawai, M. (1994) *Biophys. J.* **67,** 1655–1668.
12. Cooke, R. (1997) *Physiol. Rev.* **77,** 671–697.
13. Hill, A. V. (1938) *Proc. R. Soc. London Ser. B* **126,** 136–195.
14. Kushmerick, M. J. & Davies, R. E. (1969) *Proc. R. Soc. London Ser. B* **174,** 315–353.
15. Homsher, E., Irving, M. & Wallner, A. (1981) *J. Physiol. (London)* **321,** 423–436.
16. Woledge, R. C., Curtin, N. A. & Homsher, E. (1985) *Energetic Aspects of Muscle Contraction* (Academic, London).
17. Huxley, A. F. & Lombardi, V. (1980) *J. Physiol. (London)* **305,** 15P–16P.
18. Lombardi, V. & Piazzesi, G. (1990) *J. Physiol. (London)* **431,** 141–171.
19. Huxley, A. F., Lombardi, V. & Peachey, L. D. (1981) *J. Physiol. (London)* **317,** 12–13P.
20. Podolsky, R. J. (1960) *Nature* **188,** 666–668.
21. Huxley, A. F. (1974) *J. Physiol. (London)* **243,** 1–43.
22. Edman, K. A. & Curtin, N. A. (2001) *J. Physiol. (London)* **534,** 553–563.
23. Lombardi, V., Piazzesi, G. & Linari, M. (1992) *Nature* **355,** 638–641.
24. Linari, M., Brunello, E., Reconditi, M., Sun, Y.-B., Panine, P., Narayanan, T., Piazzesi, G., Lombardi, V. & Irving, M. (2005) *J. Physiol. (London)* **567,** 459–469.
25. Rayment, I., Holden, H. M., Whittaker, M., Yohn, C. B., Lorenz, M., Holmes, K. C. & Milligan, R. A. (1993) *Science* **261,** 58–65.
26. Geeves, M. A. & Holmes, K. C. (1999) *Annu. Rev. Biochem.* **68,** 687–728.
27. Dominguez, R., Freizon, Y., Trybus, K. M. & Cohen, C. (1998) *Cell* **94,** 559–571.
28. Huxley, A. F. & Simmons, R. M. (1971) *Nature* **233,** 533–538.
29. Piazzesi, G., Francini, F., Linari, M. & Lombardi, V. (1992) *J. Physiol. (London)* **445,** 659–711.
30. White, H. D. & Taylor, E. W. (1976) *Biochemistry* **15,** 5818–5826.
31. Dantzig, J. A., Goldman, Y. E., Millar, N. C., Lacktis, J. & Homsher, E. (1992) *J. Physiol. (London)* **451,** 247–278.